DALTON
FULL PAPER

Compounds featuring a bond between a Group 13 (M) and a Group 15 element (N or P) and with the formulae H_mMNH_n and H_mMPH_n: structural aspects and bonding

Hans-Jörg Himmel,* Anthony J. Downs, Jennifer C. Green and Tim M. Greene

Inorganic Chemistry Laboratory, University of Oxford, South Parks Road, Oxford, UK OX1 3QR

Received 30th October 2000, Accepted 9th January 2001

Following studies of the thermal and photoactivated reactions of the Group 13 metal atoms Al, Ga or In (M) with NH_3 or PH_3 in solid argon matrices, the properties of the observed or potential reaction products are discussed. These are molecules with the general formula H_mMEH_n, where M = Al, Ga or In, E = N or P, and m, n = 0–3. All the molecules have been characterised structurally, energetically and vibrationally by Density Functional Theory (DFT) calculations. The following products have been identified experimentally by their IR spectra: the adducts $M{\cdot}EH_3$, the metal(II) insertion products $HMEH_2$, the metal(III) derivatives H_2MNH_2 and H_2MPH, and the metal(I) amides MNH_2. The observation of most of the IR-active fundamentals for different isotopic forms of the molecules MNH_2 and H_2MNH_2 allowed normal coordinate analysis calculations to be performed, thereby endorsing the vibrational assignments and affording reliable force constants. Observed and hypothetical H_mMEH_n molecules have been compared with particular reference to structural and energetic differences according to whether E = N or P. Questions of bonding have been addressed through calculations of barriers to rotation of planar molecules and of barriers to inversion for molecules containing pyramidal MPH_2 moieties. π-Type interactions play only a minor part in the bonding of planar molecules like H_2MNH_2. The much larger barrier to inversion of PH_3 compared with NH_3 results in pyramidal MPH_2 but planar MNH_2 fragments. With the help of an appropriate MO scheme it is possible to rationalise how the inversion barrier changes when one hydrogen of PH_3 is replaced by an MH_m group.

Amido and phosphido derivatives of Group 13 metals are potentially relevant to the fabrication and properties of the III–V semiconductor materials AlN, AlP, GaN, GaP, InN, and InP.[1] They are normally oligomeric or polymeric, with a coordination number of 4 or greater at M; only with the introduction of bulky substituents at M and either N or P can monomeric compounds with three-coordinated M atoms be sustained under normal conditions.[2] The properties of these monomeric amido or phosphido derivatives have attracted considerable theoretical attention, mainly in relation to the potential for M–N and M–P multiple bonding.[3–5]

In two previous publications we have shown that Al, Ga or In (M) atoms react thermally with NH_3 or PH_3 on co-condensation in a solid argon matrix at 12 K to give the adducts $M{\cdot}NH_3$[6] or $M{\cdot}PH_3$.[7] Both of these are photolabile but the photoactivated matrix reactions they undergo are notably different. Irradiation into their absorption maxima near 440 nm brings about tautomerisation to the divalent species $HMNH_2$ and $HMPH_2$. No other reaction product is formed at this stage of photolysis of $M{\cdot}NH_3$. In the case of $M{\cdot}PH_3$, however, the compounds H_2MPH are also formed and, when M = Ga or In, PH is an additional product. The corresponding nitrogen product H_2MNH was not observed at any stage. Photolysis with broad-band UV–visible light ($200 \le \lambda \le 800$ nm) gives rise to two new products in the experiments with NH_3, namely the metal(III) derivative H_2MNH_2 and the metal(I) derivative MNH_2. There is clear evidence that H_2MNH_2 is formed in two steps, the first involving cleavage of the M–H bond of $HMNH_2$ to give H atoms and MNH_2, and the second H atom addition to unchanged $HMNH_2$ molecules. H_2MNH_2 and MNH_2 appear then to be photostable end-products of the reaction with ammonia (at least with respect to light having λ = 200–800 nm). The photoinduced reactions of $HMPH_2$ and H_2MPH follow different courses. Irradiation at wavelengths near 550 nm causes $HMPH_2$ to decay quickly with some accretion of PH being the only detectable outcome; meanwhile H_2MPH persists. Photolysis with UV light (λ = 200–400 nm) brings about the decay of H_2MPH but without the emergence of a product identifiable by its IR spectrum.

The different reaction pathways having been established,[6,7] we focus here on the properties of the observed H_mMNH_n and H_mMPH_n products (m, n = 0–3) which have been characterised by their IR spectra, the conclusions being underpinned by the effects of isotopic change and by comparison with the vibrational properties anticipated by Density Functional Theory (DFT) calculations. We start with a normal mode analysis of MNH_2 and H_2MNH_2. All the observed products are then compared for structure, energy and vibrational properties, not only with one another but also with hypothetical products having the general formula H_mMEH_n (E = N or P). This is achieved on the basis of DFT calculations and of applying the B3LYP method which has been shown previously to give a good account of small aluminium and gallium compounds.[8] The question of bonding is investigated by calculating (i) the barriers to rotation about the M–E bond in planar molecules, and (ii) the barriers to inversion of MEH_2 fragments.

Experimental

Experimental details of the matrix studies are given elsewhere.[6,7]

Density Functional Theory calculations were performed using the GAUSSIAN 98 program package[9] and applying the B3LYP method, as described previously.[6,7] A 6-311G(d) basis set was used for Al and Ga, a LANL2DZ basis set with additional d-polarisation functions (exponent 0.5) for In. Orbital analysis was performed on PH_3 and H_2GaPH_2 using the Amsterdam Density Functional code (ADF 2000.02).[10] The

DOI: 10.1039/b008724f

basis set used type V basis sets with triple-ζ accuracy sets of Slater type orbitals with polarisation functions. The GGA (non-local) method was used, employing Vosko, Wilk and Nusair's local exchange correlation,[11] with non-local-exchange corrections by Becke,[12] and non-local correlation corrections by Perdew.[13,14] Relativistic corrections were made using the ZORA method. Calculated geometries and frequencies were in good agreement with those obtained using GAUSSIAN 98.

Normal coordinate analysis (NCA) calculations were carried out with the aid of the program ASYM 40.[15]

Results

Table 1 summarises the experimental and calculated frequencies for all the compounds identified in the matrix experiments.[6,7] The observed frequencies for other isotopomers can be found elsewhere,[6,7] or, in the cases of MNH_2 (M = Al, Ga or In) and H_2MNH_2 (M = Al or Ga), in the respective Tables 2 and 3, which include the results of the normal coordinate analysis calculations.

Normal mode analysis

The observation of a nearly complete set of IR fundamentals for each of the molecules MNH_2 (M = Al, Ga or In) and H_2MNH_2 (M = Al or Ga) in different isotopic forms invites a normal mode analysis. Based on the program ASYM 40,[15] the results of such an analysis, included in Tables 2 and 3, lend strong support to the assignments given in Table 1. The dimensions have been taken from the DFT-calculated structures as detailed in Table 1. For all five molecules the observed frequencies for the fundamentals involving motions of the hydrogen atoms have been harmonised using two anharmonicity constants x_i, where $\nu_i = \omega_i(1 - x_i)$; these are $x_i = 0.035$ for hydrogen stretching and $x_i = 0.020$ for angle deformation. For the other isotopic species Dennison's rule[16] was applied such that $x_i' = x_i\nu_i'/\nu_i$. Such an approach has proved successful in the analysis of the vibrational spectra of $[H_2GaCl]_2$,[17] $HInCl_2$[18] and H_2InCl.[18] The symmetry coordinates used in the refinement are given in Tables 2 and 3 along with the values derived for the force constants. The general level of agreement is extremely pleasing and only in two cases is there a significant discrepancy between the observed frequencies that have been scaled and those afforded by the normal coordinate analysis. The first of these occurs with the b_1 mode of $GaND_2$ while the second occurs in the b_2 block of $InNH_2$. In both cases the problem arises because the observed frequencies, even after scaling, are significantly different from those delivered by the DFT calculations. This may arise in part from varying degrees of anharmonicity for the different modes that cannot adequately be accommodated by our relatively simple correction method. The data set being incomplete, the NCA calculations must then be carried out with a combination of these two sets of frequencies, and unfortunately the fit is then a relatively poor one. To allow for comparison, the Cartesian force constants resulting from the DFT calculations have been transformed to a set of constants corresponding to the symmetry coordinates. On the evidence of Tables 2 and 3 the values are in reasonable agreement.

For none of the other molecules identified by experiment has it been feasible or worthwhile to attempt a similar analysis, whether for lack of a sufficient number of observed IR features or for lack of symmetry of the molecule in question (resulting in poor definition of particular types of vibrational motion).

Properties of H_mMNH_n and H_mMPH_n compounds (m, n = 0–3)

Tables 4 and 5 include both calculated and, where available, experimental results for compounds with the general formula H_mMNH_n and H_mMPH_n (m, n = 0–3).

$M{\cdot}NH_3$ and $M{\cdot}PH_3$. Adducts of both these types have been identified in matrix experiments by their IR spectra.[6,7] DFT calculations find a global minimum for such a molecule with the geometry **1a** and **1b**; the optimised dimensions and vibrational properties are included in Tables 4 and 5. As expected on the basis of earlier theoretical studies of $Al{\cdot}EH_3$ (E = N[3,4] or P[4,5]), each of the molecules deviates slightly from regular C_{3v} symmetry. This is achieved through one E–H bond being slightly shorter than the other two and the H–E–H angles being fractionally different, so that the overall symmetry is C_s, and there are as a result not 6 but 9 distinct vibrational fundamentals.

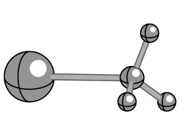

1a ($M{\cdot}NH_3$)

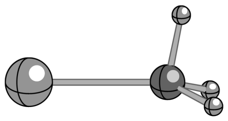

1b ($M{\cdot}PH_3$)

At 2.3344, 2.4560 and 2.7084 Å for M = Al, Ga or In, respectively, the M–N distances are about 1 Å shorter than the sums of the relevant van der Waals radii.[19] The corresponding $M \cdots P$ distances are 2.7755, 2.8411 and 3.2219 Å, shorter than the sums of the van der Waals radii by margins ranging from 1.2 Å for M = Al to 0.6 Å for M = In. The estimated binding energies (in kJ mol^{-1} and in the order Al, Ga and In) are 60.2, 51.8 and 28.8 for $M{\cdot}NH_3$, and 21.8, 22.1 and 17.0 for $M{\cdot}PH_3$. The ligand–metal atom interactions thus increase in the order $M{\cdot}N_2$[20] < $M{\cdot}PH_3$ < $M{\cdot}NH_3$ < $M{\cdot}CO$,[21] the binding energies in the case of M = Al being 16.4, 21.8, 60.2 and 81 kJ mol^{-1}, respectively.

The most prominent feature in the IR spectrum of each adduct $M{\cdot}EH_3$ is ν_2 (a′) corresponding to the symmetric EH_3 deformation and occurring near 1100 cm^{-1} for E = N or near 970 cm^{-1} for E = P (see Table 6). Here the spectra show *blue* shifts of 100–160 cm^{-1} for $M{\cdot}NH_3$ with respect to ν_2 of free NH_3 but *red* shifts of about 20 cm^{-1} for $M{\cdot}PH_3$ with respect to ν_2 of free PH_3. This feature is well anticipated by the DFT calculations. Hence there appears to be a significant difference in not only the strength but also the *nature* of the $M \cdots EH_3$ interaction according to whether E = N or P.

$HMNH_2$ and $HMPH_2$. Photolysis of the adduct $M{\cdot}EH_3$ with light at wavelengths near 440 nm results in tautomerisation to form the insertion product $HMEH_2$ containing a metal(II) centre for both E = N and E = P. DFT calculations find equilibrium geometries for $HAlNH_2$ and $HGaNH_2$ which are significantly different from those of $HMPH_2$ (M = Al, Ga or In), the former being planar at nitrogen (with C_s symmetry), the latter pyramidal at phosphorus (and therefore belonging to the C_1 point group), as pictured in structures **2a** and **2b**. Curiously the equilibrium structure of $HInNH_2$ is found to feature an $InNH_2$ fragment with a geometry intermediate between those of the planar units of $HAlNH_2$ and $HGaNH_2$ and the decidedly pyramidal ones of $HMPH_2$. The vibrational properties computed reproduce well the features observed in the IR spectra of all six molecules.

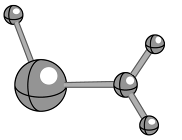

2a ($HMNH_2$)

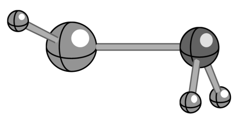

2b ($HMPH_2$)

The structural differences between the amido and phosphido derivatives are in keeping with the very different barriers to

Table 1 Observed and calculated vibrational wavenumbers (cm^{-1}) for the products of the photo-induced matrix reactions between Al (a), Ga (b) or In (c) and EH_3 (E = N or P)

NH_3			PH_3			
exp.	calc.[a]	assignment	exp.	calc.[a]	assignment	Absorber
(a)						
3447.1	3573.1 (43)	ν_{asym} (N–H)	2285.5	2334.7 (375)	ν_{sym}(P–H)	$Al\cdot EH_3$
1593.6	1600.1 (20)	δ_{asym} (NH_3)	1101.2	1156.2 (101)	ν_{asym}(P–H)	
1131.4	1231.0 (174)	δ_{sym}(NH_3)	974.7	1025.1 (137)	δ_{sym}(PH_3)	
3476.4	3645.1 (14)	ν_{sym}(N–H)	1768.2	1826.7 (260)	ν(Al–H)	$HAlEH_2$
1761.1	1820.5 (205)	ν(Al–H)	1159.4	1120.8 (19)	PH_2 scissoring	
1533.6	1620.4 (41)	NH_2 scissoring	727.1	691.0 (33)	PH_2 wagging	
778.7	795.0 (86)	ν(Al–N)	[b]	452.9 (22)	PH_2 *out-of-plane* rock	
705.2	746.9 (116)	NH_2 wagging	403.9	426.3 (55)	Al–H *in-plane* def.	
482.2	486.5 (27)	Al–H *in-plane* def.				
483.8	498.3 (31)	NH_2 *out-of-plane* rock				
393.8	426.5 (226)	Al–H *out-of-plane* def.				
1520.3	1614.0 (63)	NH_2 scissoring				$AlEH_2$
726.5	735.1 (81)	ν(Al–N)				
406.5	469.3 (263)	*out-of-plane* def.				
3495.1	3590.3 (6)	ν_{asym}(N–H)				
			1874.7	1953.2 (244)	ν_{asym}(Al–H)	H_2AlEH
			1866.1	1936.9 (168)	ν_{sym}(Al–H)	
			765.9	781.8 (349)	AlH_2 bend	
			606.3	670.0 (36)	H–P–Al bend	
			569.0	518.9 (179)	AlH_2 wagging	
3499.7	3572.0 (11)	ν_{sym}(N–H)				H_2AlEH_2
1891.0	1959.3 (81)	ν_{sym}(Al–H)				
1541.6	1631.2 (49)	δ(NH_2)				
818.7	830.1 (192)	ν(Al–N)				
755.0	754.6 (86)	δ(AlH_2)				
608.7	608.4 (150)	$\rho_{out\text{-}of\text{-}plane}$($AlH_2$)				
518.3	483.0 (309)	$\rho_{out\text{-}of\text{-}plane}$($NH_2$)				
[b]	3655.8 (11)	ν_{asym}(N–H)				
1899.3	1964.2 (288)	ν_{asym}(Al–H)				
769.8	767.6 (151)	$\delta_{in\text{-}plane}$(NH_2)				
(b)						
3441.5	3594.3 (29)	ν_{asym} (N–H)	2280.8	2346.8 (316)	ν_{sym}(P–H)	$Ga\cdot EH_3$
1580.7	1590.6 (12)	δ_{asym} (NH_3)	1108.2	1158.7 (86)	δ_{asym}(PH_3)	
1104.2	1189.4 (153)	δ_{sym}(NH_3)	973.6	1025.7 (141)	δ_{sym}(PH_3)	
1721.8	1759.3 (189)	ν(Ga–H)	1721.4	1740.6 (303)	ν(Ga–H)	$HGaEH_2$
1528.7	1601.3 (21)	NH_2 scissoring	1060.9	1122.0 (19)	PH_2 scissoring	
746.2	752.2 (78)	NH_2 wagging	428.2	412.9 (33)	Ga–H *in-plane* def.	
668.5	665.0 (59)	ν(^{69}Ga–N)				
494.1	481.0 (21)	NH_2 *out-of-plane* rock				
210.9	229.1 (238)	Ga–H *out-of-plane* def.				
1505.9	1599.9 (32)	NH_2 scissoring				$GaEH_2$
589.3	595.2 (94)	ν(^{69}Ga–N)				
303.3	363.5 (283)	*out-of-plane* def.				
3471.6	3599.7 (2)	ν_{asym} (N–H)				
			1897.5	1960.4 (239)	ν_{asym}(Ga–H)	H_2GaEH
			1893.3	1948.2 (167)	ν_{sym}(Ga–H)	
			738.9	735.4 (229)	GaH_2 bend	
			646.5	673.7 (23)	H–P–Ga bend	
			454.8	501.0 (84)	GaH_2 wagging	
3413.4	3581.9 (9)	ν_{sym}(N–H)				H_2GaEH_2
1970.8	1995.9 (64)	ν_{sym}(Ga–H)				
1530.4	1621.6 (30)	δ(NH_2)				
779.6	740.3 (40)	δ(GaH_2)				
706.2	689.0 (124)	ν(^{69}Ga–N)				
567.7	607.9 (43)	$\rho_{out\text{-}of\text{-}plane}$($GaH_2$)				
304.9	337.3 (280)	$\rho_{out\text{-}of\text{-}plane}$($NH_2$)				
3510.7	3681.7 (13)	ν_{asym}(N–H)				
1970.8	1998.6 (245)	ν_{asym}(Ga–H)				
782.8	789.8 (110)	$\delta_{in\text{-}plane}$(NH_2)				
(c)						
3424.4	3542.3 (24)	ν_{asym}(N–H)	1105.7	1167.5 (40)	δ_{asym}(PH_3)	$In\cdot EH_3$
1082.9	1171.7 (133)	δ_{sym}(NH_3)	974.4	1042.0 (146)	δ_{sym}(PH_3)	

Table 1 (*Contd.*)

NH_3			PH_3			
exp.	calc.[a]	assignment	exp.	calc.[a]	assignment	Absorber
3463.5	3597.6 (15)	ν_{sym}(N–H)	2299.4	2373.3 (55)	ν_{asym}(P–H)	$HInEH_2$
1533.8	1580.6 (197)	ν(In–H)	1546.4	1570.4 (320)	ν(In–H)	
1512.9	1567.7 (28)	NH_2 scissoring				
709.0	682.5 (97)	NH_2 wagging				
564.8	555.9 (57)	ν(In–N)				
1498.1	1568.1 (26)	NH_2 scissoring				$InEH_2$
498.7	504.3 (93)	ν(In–N)				
237.0	256.3 (236)	*out-of-plane* def.				
3481.7	3548.3 (4)	ν_{asym}(N–H)				
469.6	447.8 (3)	$\rho(NH_2)$				
			674.7	634.8 (304)	H–P–In bend	H_2InEH
1506.6	1579.4 (23)	$\delta(NH_2)$				H_2InEH_2
616.3	575.8 (153)	ν(In–N)				
1805.9	1756.9 (272)	ν_{asym}(In–H)				
733.3	696.3 (126)	$\delta_{in\text{-}plane}(NH_2)$				

[a] Values taken from DFT calculations; IR intensities (in km mol^{-1}) given in parentheses. [b] Not observed.

Table 2 Normal coordinate analysis for $M^{14}NH_2/M^{15}NH_2/M^{14}ND_2$ [M = Al (a), Ga (b) or In (c)] and comparison with the wavenumbers (in cm^{-1}) and force constants calculated by DFT methods

	$M^{14}NH_2$			$M^{15}NH_2$			$M^{14}ND_2$		
Mode	ν_i	ω_i	calc.[a]	ν_i	ω_i	calc.[a]	ν_i	ω_i	calc.[a]
(a)									
ν_1 (a_1)	[b]	3503.7[a]	3503.7	[b]	3498.6[a]	3498.6	[b]	2534.6[a]	2534.6
ν_2 (a_1)	1520.3	1551.3	1614.0	1515.0	1545.8	1608.7	1137.8	1155.1	1202.6
ν_3 (a_1)	726.5	726.5	735.1	713.6	713.6	721.9	694.9	694.9	698.2
ν_4 (b_1)	406.5	414.8	469.3	403.9	412.1	466.2	314.6	319.5	364.7
ν_5 (b_2)	3495.1	3621.9	3590.3	3486.2	3612.3	3580.4	[b]	2643.5[a]	2643.5
ν_6 (b_2)	[b]	499.0[a]	499.0	[b]	496.8[a]	496.8	[b]	377.4[a]	377.4
(b)									
ν_1 (a_1)	[b]	3499.8[c]	3499.8	[b]	3494.2[c]	3494.2	[b]	2528.7[c]	2528.7
ν_2 (a_1)	1505.9	1536.6	1599.9	1501.2	1531.7	1595.0	1132.6	1149.8	1189.5
ν_3 (a_1)	589.3	589.3	595.2	574.3	574.3	581.0	557.9	557.9	560.8
ν_4 (b_1)	303.3	309.5	363.5	302.7	308.9	362.7	[b]	282.5[c]	282.5
ν_5 (b_2)	3471.6	3597.5	3599.7	[b]	3588.7[c]	3588.7	[b]	2652.1[c]	2652.1
ν_6 (b_2)	[b]	509.0[c]	509.0	[b]	507.3[c]	507.3	[b]	382.4[c]	382.4
(c)									
ν_1 (a_1)	[b]	3446.0[d]	3446.0	[b]	3441.2[d]	3441.2	[b]	2490.6[d]	2490.6
ν_2 (a_1)	1498.1	1528.7	1568.1	1493.6	1524.0	1563.3	1116.3	1133.2	1160.8
ν_3 (a_1)	498.7	498.7	504.3	488.2	488.2	491.3	480.6	480.6	475.3
ν_4 (b_1)	237.0	241.8	256.3	235.4	240.2	254.6	[b]	198.3[d]	198.3
ν_5 (b_2)	3481.7	3608.0	3548.3	[b]	3538.4[d]	3538.4	[b]	2613.3[d]	2613.3
ν_6 (b_2)	469.6	479.2	447.8	[b]	445.9[d]	445.9	[b]	335.1[d]	335.1

[a] Values taken from DFT calculations. R = Al–N, r = N–H, α = H–N–H, β = Al–N–H, $S_1 = \delta r_1 + \delta r_2$, $S_2 = 2\delta\alpha - \delta\beta_1 - \delta\beta_2$, $S_3 = \delta R$, $S_4 = \delta\tau$, $S_5 = \delta r_1 - \delta r_2$, $S_6 = \delta\beta_1 - \delta\beta_2$. Force constant values (stretching constants in N m^{-1}, bending constants in 10^{-20} J, stretch–bend constants in 10^{-10} N): (a) NCA $F_{1,1}$ 699.6, $F_{1,2}$ 23.1, $F_{1,3}$ 17.7, $F_{2,2}$ 45.9, $F_{2,3}$ −10.0, $F_{3,3}$ 313.5, $F_{4,4}$ 5.7, $F_{5,5}$ 716.8, $F_{5,6}$ 42.8; $F_{6,6}$ 15.1; (b) DFT $F_{1,1}$ 697.1, $F_{1,2}$ 18.0, $F_{1,3}$ 6.3, $F_{2,2}$ 48.9, $F_{2,3}$ −6.2, $F_{3,3}$ 321.7, $F_{4,4}$ 7.3, $F_{5,5}$ 701.6, $F_{5,6}$ 11.8, $F_{6,6}$ 12.9. [b] Not observed. [c] R = Ga–N, β = Ga–N–H, other details are in footnote *a*. Force constant values: (a) NCA $F_{1,1}$ 703.3, $F_{1,2}$ 11.6, $F_{1,3}$ 62.5, $F_{2,2}$ 43.8, $F_{2,3}$ −1.1, $F_{3,3}$ 272.4, $F_{4,4}$ 3.4, $F_{5,5}$ 703.4, $F_{5,6}$ 8.4, $F_{6,6}$ 13.6; (b) DFT $F_{1,1}$ 696.0, $F_{1,2}$ 19.8, $F_{1,3}$ 4.5, $F_{2,2}$ 48.1, $F_{2,3}$ −4.8, $F_{3,3}$ 272.5, $F_{4,4}$ 4.4, $F_{5,5}$ 703.7, $F_{5,6}$ 8.6, $F_{6,6}$ 13.6. [d] R = In–N, β = In–N–H, other details as in footnote *a*. Force constant values: (a) NCA $F_{1,1}$ 675.5, $F_{1,2}$ 49.4, $F_{1,3}$ 25.3, $F_{2,2}$ 49.4, $F_{2,3}$ −15.4, $F_{3,3}$ 210.0, $F_{4,4}$ 2.1, $F_{5,5}$ 668.9, $F_{5,6}$ −55.9, $F_{6,6}$ 16.1; (b) DFT $F_{1,1}$ 674.2, $F_{1,2}$ 21.7, $F_{1,3}$ 2.8, $F_{2,2}$ 47.2, $F_{2,3}$ −5.0, $F_{3,3}$ 211.2, $F_{4,4}$ 2.3, $F_{5,5}$ 685.1, $F_{5,6}$ 7.9, $F_{6,6}$ 10.8.

inversion of the parent molecules NH_3[30] and PH_3,[31] which can in turn be explained, for example, through second-order Jahn–Teller arguments.[32] Table 7 lists some representative barriers to inversion; only for NH_3 and PH_3 are experimental estimates available but these are in fair agreement with the results of DFT calculations. Thus the replacement of an H atom of PH_3 by HM leads to a decrease of the barrier to inversion (from 148.2 kJ mol^{-1} for PH_3 to 42.6, 56.7 and 59.2 kJ mol^{-1} for $HMPH_2$, where M = Al, Ga or In, respectively).

For the $HMNH_2$ compounds the barriers to rotation for the planar structures have been calculated with transition states each exhibiting a planar NH_2 fragment orthogonal to the HMN plane. Two imaginary frequencies were obtained for the transition states. The M–N, M–H and N–H bond lengths (in Å) in the transition states are 1.8086, 1.6224, 1.0114 for M = Al, 1.8726, 1.6332, 1.0107 for M = Ga and 2.0190, 1.7936, 1.0191 for M = In. The barriers to rotation are 38.7, 37.6 and 31.3 kJ mol^{-1}.

Table 3 Normal coordinate analysis for $H_2M^{14}NH_2/H_2M^{15}NH_2/H_2M^{14}ND_2$ [M = Al (a) or Ga (b)] and comparison with the wavenumbers (in cm^{-1}) and force constants calculated by DFT methods

	$H_2M^{14}NH_2$			$H_2M^{15}NH_2$			$H_2M^{14}ND_2$		
Mode	ν_i	ω_i	calc.[a]	ν_i	ω_i	calc.[a]	ν_i	ω_i	calc.[a]
(a)									
ν_1 (a_1)	3499.7	3626.6	3572.0		3566.9[b]	3566.9		2583.9[b]	2583.9
ν_2 (a_1)	1891.0	1959.6	1959.3	1891.1	1959.7	1959.3		1398.2[b]	1398.2
ν_3 (a_1)	1541.6	1573.1	1631.2	1536.1	1567.3	1625.8	1159.5	1177.2	1218.0
ν_4 (a_1)	818.7	818.7	830.1	809.8	809.8	820.2		774.1[b]	774.1
ν_5 (a_1)	755.0	770.4	754.6		749.6[b]	749.6	548.4	556.5	548.7
ν_6 (a_2)	[c]			[c]			[c]		
ν_7 (b_1)	608.7	621.1	608.4	608.1	620.5	608.4	450.4	457.2	455.5
ν_8 (b_1)	518.3	528.9	483.0	516.7	527.2	479.6	397.7	403.9	376.9
ν_9 (b_2)		3655.8[b]	3655.8		3645.5[b]	3645.5		2694.5[b]	2694.5
ν_{10} (b_2)	1899.3	1968.2	1964.2	1899.3	1968.2	1964.2	1384.2	1420.4	1426.6
ν_{11} (b_2)	769.8	785.5	767.6	766.2	781.4	762.9	591.7	600.9	603.4
ν_{12} (b_2)		433.5[b]	433.5		433.5[b]	433.5		311.7[b]	311.7
(b)[d]									
ν_1 (a_1)	3413.4	3537.2	3581.9	3405.9	3529.1	3577.0		2588.3[b]	2588.3
ν_2 (a_1)	1970.8	2042.3	1995.9	1970.7	2042.2	1995.9	1407.7	1443.8	1415.6
ν_3 (a_1)	1530.4	1561.6	1621.6	1524.3	1555.3	1616.2	1150.9	1168.5	1208.6
ν_4 (a_1)	779.6	795.5	740.3	775.2	790.9	736.8	568.8	577.2	519.8
ν_5 (a_1)	706.2	706.2	689.0	692.2	692.2	675.9	667.8	667.8	658.0
ν_6 (a_2)	[c]			[c]			[c]		
ν_7 (b_1)	567.7	579.3	607.9	567.4	578.9	607.9	405.9	411.8	439.7
ν_8 (b_1)	304.9	311.1	337.3	302.8	308.9	334.9		263.3[b]	263.3
ν_9 (b_2)	3510.7	3638.0	3681.7	3500.7	3627.3	3670.9		2717.3[b]	2717.3
ν_{10} (b_2)	1970.8	2042.3	1998.6	1970.7	2042.2	1998.5	1419.1	1455.8	1428.3
ν_{11} (b_2)	782.8	798.8	789.8	778.3	794.1	785.1	605.1	614.6	608.8
ν_{12} (b_2)		441.8[b]	441.8		441.7[b]	441.7		316.2[b]	316.2

[a] Values taken from DFT calculations. R = Al–N, r = Al–H, r' = N–H, α = H–Al–H, β = N–Al–H, α' = H–N–H, β' = Al–N–H, τ_0 = HAlNH, $S_1 = \delta r_1' + \delta r_2'$, $S_2 = \delta r_1 + \delta r_2$, $S_3 = 2\delta\alpha' - \delta\beta_1' - \delta\beta_2'$, $S_4 = \delta R$, $S_5 = 2\delta\alpha - \delta\beta_1 - \delta\beta_2$, $S_6 = \delta\tau_3 - \delta\tau_4$, $S_7 = \delta\tau_1$, $S_8 = \delta\tau_2$, $S_9 = \delta r_1' - \delta r_2'$, $S_{10} = \delta r_1 - \delta r_2$, $S_{11} = \delta\beta_1' - \delta\beta_2'$, $S_{12} = \delta\beta_1 - \delta\beta_2$. Force constant values (stretching constants in N m^{-1}, bending and torsion constants in 10^{-20} J, stretch–bend and stretch–torsion constants in 10^{-10} N): (a) NCA $F_{1,1}$ 731.1, $F_{1,2}$ 4.8, $F_{1,3}$ −4.9, $F_{1,4}$ −32.8, $F_{1,5}$ 7.3, $F_{2,2}$ 224.7, $F_{2,3}$ −3.6, $F_{2,4}$ 11.1, $F_{2,5}$ 3.4, $F_{3,3}$ 44.9, $F_{3,4}$ −3.2, $F_{3,5}$ 1.2, $F_{4,4}$ 408.2, $F_{4,5}$ −8.7, $F_{5,5}$ 28.5, $F_{7,7}$ 17.1, $F_{7,8}$ 2.8, $F_{8,8}$ 8.7, $F_{9,9}$ 725.3, $F_{9,10}$ −5.7, $F_{9,11}$ 12.4, $F_{9,12}$ 4.0, $F_{10,10}$ 216.4, $F_{10,11}$ −6.6, $F_{10,12}$ −1.5, $F_{11,11}$ 31.2, $F_{11,12}$ −0.2, $F_{12,12}$ 23.2; (b) DFT $F_{1,1}$ 725.2, $F_{1,2}$ 0.0, $F_{1,3}$ 16.9, $F_{1,4}$ 4.5, $F_{1,5}$ −0.8, $F_{2,2}$ 224.6, $F_{2,3}$ −1.6, $F_{2,4}$ 9.2, $F_{2,5}$ 2.6, $F_{3,3}$ 49.5, $F_{3,4}$ −10.0, $F_{3,5}$ 0.3, $F_{4,4}$ 398.2, $F_{4,5}$ −6.4, $F_{5,5}$ 28.3, $F_{6,6}$ 7.5, $F_{7,7}$ 20.4, $F_{7,8}$ 2.0, $F_{8,8}$ 5.9, $F_{9,9}$ 726.5, $F_{9,10}$ 0.5, $F_{9,11}$ 12.4, $F_{9,12}$ −4.0, $F_{10,10}$ 216.9, $F_{10,11}$ −1.3, $F_{10,12}$ 5.4, $F_{11,11}$ 22.8, $F_{11,12}$ −10.0, $F_{12,12}$ 35.0. [b] No experimentally observed frequency; value taken from DFT calculations. [c] IR inactive. [d] R = Ga–N, r = Ga–H, α = H–Ga–H, β = N–Ga–H, β' = Ga–N–H, τ_0 = HGaNH, $S_4 = 2\delta\alpha - \delta\beta_1 - \delta\beta_2$, $S_5 = \delta R$, other details as in footnote *a*. Force constant values: (a) NCA $F_{1,1}$ 708.5, $F_{1,2}$ 3.1, $F_{1,3}$ −5.4, $F_{1,4}$ −10.4, $F_{1,5}$ −10.1, $F_{2,2}$ 244.6, $F_{2,3}$ −2.8, $F_{2,4}$ −6.0, $F_{2,5}$ −3.3, $F_{3,3}$ 44.3, $F_{3,4}$ 2.3, $F_{3,5}$ −1.4, $F_{4,4}$ 30.6, $F_{4,5}$ −3.2, $F_{5,5}$ 397.0, $F_{7,7}$ 17.9, $F_{7,8}$ 1.0, $F_{8,8}$ 2.5, $F_{9,9}$ 721.7, $F_{9,10}$ −4.8, $F_{9,11}$ 13.1, $F_{9,12}$ 7.2, $F_{10,10}$ 241.5, $F_{10,11}$ −4.6, $F_{10,12}$ −1.7, $F_{11,11}$ 32.8, $F_{12,12}$ −1.2, $F_{12,12}$ 25.5; (b) DFT $F_{1,1}$ 730.0, $F_{1,2}$ −0.2, $F_{1,3}$ 17.6, $F_{1,4}$ −1.4, $F_{1,5}$ 2.5, $F_{2,2}$ 235.3, $F_{2,3}$ −1.9, $F_{2,4}$ 5.6, $F_{2,5}$ 7.2, $F_{3,3}$ 48.8, $F_{3,4}$ 1.3, $F_{3,5}$ −10.3, $F_{4,4}$ 25.4, $F_{4,5}$ −11.9, $F_{5,5}$ 381.9, $F_{6,6}$ 9.1, $F_{7,7}$ 19.6, $F_{7,8}$ 2,8, $F_{8,8}$ 3.2, $F_{9,9}$ 734.2, $F_{9,10}$ 0.5, $F_{9,11}$ 9.1, $F_{9,12}$ −3.3, $F_{10,10}$ 232.2, $F_{10,11}$ −2.1, $F_{10,12}$ 11.0, $F_{11,11}$ 27.2, $F_{11,12}$ −9.8, $F_{12,12}$ 33.7.

In the same way the barriers to rotation of the planarised $HMPH_2$ compounds were calculated to gain further information about the strength of the π bonding; in the transition state the molecules exhibit C_s geometry and the PH_2 fragment is constrained to be planar. The M–P, M–H and P–H distances (in Å) in these transition states are 2.3387, 1.6132, 1.4050 for M = Al, 2.6145, 1.6704, 1.4179 for M = Ga, and 2.9723, 1.8444, 1.4219 for M = In. The barriers to rotation for the planarised structures are 47.9, 35.0 and 23.9 kJ mol^{-1} for M = Al, Ga or In, respectively.

The dimensions and vibrational properties of $HMNH_2$ and $HMPH_2$ also invite comparison with those of other derivatives of the divalent Group 13 metals, *e.g.* MH_2,[39] CH_3MH[40,41] and HMOH,[42] with the results given in Table 8. Hence it emerges that the stretching force constants f_{MX} for molecules of the type HMX vary in the order Al > Ga > In, and that for a given metal with some vacant valence orbitals the order is typically $f_{MC} < f_{MN} \approx f_{MO}$, consistent with, but by no means establishing, a measure of N or O to M π bonding.

H_2MNH_2 and H_2MPH_2. Whereas molecules of the type H_2MNH_2 are formed *via* UV irradiation of argon matrices containing $HMNH_2$, the corresponding phosphorus compounds H_2MPH_2 have not been detected as analogous products of photodecomposition of $HMPH_2$.[7] Both types of molecule are of particular note through being formally isoelectronic with ethene and its heavier congeners like H_2SiCH_2 and H_2SiSiH_2.[46] Accordingly it is natural to enquire about the skeletal geometries and the extent of M←E π-type interaction which is optimised for a planar H_2MEH_2 skeleton.

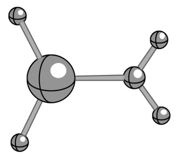
3a (H_2MNH_2)

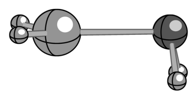
3b (H_2MPH_2)

In the case of H_2MNH_2 (M = Al, Ga or In), DFT calculations indicate that the ground state is indeed characterised by a planar, ethene-like structure having C_{2v} symmetry (see structure **3a** and Table 4) and with vibrational properties anticipating closely the observed IR spectra.[6] The structure in each case is thus analogous to that deduced previously by both theory and experiment for the corresponding boron compound H_2BNH_2;[47] there is also good agreement with the results of earlier calculations on H_2AlNH_2 (using, for example, SCF methods and CISD and CCSD levels of theory).[3]

The calculated M–N distances are indeed short, being near or below the lower limits for the observed distances in three-coordinated amido derivatives of the relevant metal (1.78, 1.818

Table 4 M–H and M–N bond lengths (Å), wavenumbers (cm^{-1}) and stretching force constants (N m^{-1}) for compounds with the formula H_mMNH_n (m = 0–3, n = 0–3; M = Al, Ga or In)

Compound	Symmetry	M–N	M–H	ν(M–N) calc.	*f*(MN) calc.	ν(M–N) exp.	*f*(MN) exp.	ν(M–H) calc.	*f*(MH) calc.	ν(M–H) exp.	*f*(MH) exp.
$Al\cdot NH_3$	C_s	2.3344		244.8	36.9						
$H_3Al\cdot NH_3$	C_s	2.0931	1.6006	403.2	104.1			1887.1 (a′), 1867.7 (a″), 1867.4 (a′)	203.2		
$AlNH_2$	C_{2v}	1.8131		735.1	321.7	726.5	313.5				
$HAlNH_2$	C_s	1.7880	1.6050	795.0	379.5	778.7	364.1	1820.5	192.3	1761.1	180.0
H_2AlNH_2	C_{2v}	1.7790	1.5811	830.1	398.2	818.7	408.1	1964.2 (b$_2$), 1959.3 (a$_1$)	220.8	1899.3, 1891.0	220.5
AlN	$C_{\infty v}$	1.8001		742.9	299.8						
HAlNH	C_s	1.6271	1.5532	1127.9	732.5			2078.1	250.5		
$Ga\cdot NH_3$	C_s	2.4560		206.2	34.3						
$H_3Ga\cdot NH_3$	C_s	2.1795	1.5823	319.3	82.9			1919.4 (a′), 1901.4 (a′), 1900.2 (a″)	213.3		
$GaNH_2$	C_{2v}	1.8840		595.2	272.5	589.3	272.4				
$HGaNH_2$	C_s	1.8360	1.6020	665.0	340.4	668.5	344.0	1759.3	181.7	1721.8	174.0
H_2GaNH_2	C_{2v}	1.8211	1.5621	689.0	381.9	706.2	397.0	1998.6 (b$_2$), 1995.9 (a$_1$)	233.8	1970.8, 1970.8	243.0
GaN	$C_{\infty v}$	1.8640		586.2	236.2						
HGaNH	C_s	1.6989	1.5276	903.3	595.5			2052.0	247.1		
$In\cdot NH_3$	C_s	2.7084		157.8	21.8						
$H_3In\cdot NH_3$	C_s	2.3788	1.7474	259.9	59.2			1716.1 (a′), 1684.2 (a′), 1683.9 (a″)	168.3		
$InNH_2$	C_{2v}	2.0389		504.3	211.2	498.7	209.9				
$HInNH_2$	C_1	1.9929	1.7676	555.9	256.3	564.8	264.6	1580.6	147.2	1533.8	138.6
H_2InNH_2	C_{2v}	1.9703	1.7252	575.8	275.3	616.3	315.3	1756.9 (b$_2$), 1770.2 (a$_1$)	181.9	1805.9	192.2
InN	$C_{\infty v}$	2.0256		501.2	184.8						
HInNH	C_s	1.8345	1.6902	768.5	462.5			1854.1	202.6		

Table 5 M–H and M–P bond lengths (Å) and stretching wavenumbers (cm^{-1}) for compounds with the formula H_mMPH_n (m = 0–3, n = 0–3; M = Al, Ga or In)

Compound	Symmetry	M–P	M–H	ν(M–P) calc.	ν(M–H) calc.	ν(M–H) exp.
$Al\cdot PH_3$	C_s	2.7755		135.9		
$H_3Al\cdot PH_3$	C_{3v}	2.5771	1.595	224.7	1901.5 (a$_1$) 1892.5 (e)	
$AlPH_2$	C_s	2.4490		378.3		
$HAlPH_2$	C_s	2.3713	1.6065	372.8	1826.7	1768.2
H_2AlPH_2	C_s	2.3379	1.5837	408.0	1957.2 (a″) 1942.9 (a′)	
AlP	$C_{\infty v}$	2.2290		454.8		
HAlPH	C_s	2.1535	1.5794	522.1	1960.0	
$Ga\cdot PH_3$	C_s	2.8411		110.9		
$H_3Ga\cdot PH_3$	C_{3v}	2.6012	1.5765	168.4	1937.9 (a$_1$) 1926.2 (e)	
$GaPH_2$	C_s	2.4829		229.0		
$HGaPH_2$	C_s	2.3919	1.6117	292.6	1740.6	1721.4
H_2GaPH_2	C_s	2.3310	1.5704	339.7	1972.5 (a″) 1959.4 (a′)	
GaP	$C_{\infty v}$	2.2616		345.7		
HGaPH	C_s	2.1445	1.5586	451.7	1986.4	
$In\cdot PH_3$	C_s	3.2219		79.2		
$H_3In\cdot PH_3$	C_{3v}	2.9351	1.7397	124.2	1735.5 (a$_1$) 1704.5 (e)	
$InPH_2$	C_s	2.6962	1.4317	226.6		
$HInPH_2$	C_1	2.6031	1.7762	244.0	1570.4	1546.4
H_2InPH_2	C_s	2.5355	1.7328	283.1	1732.0 (a″) 1736.4 (a′)	
InP	$C_{\infty v}$	2.4662		280.2		
HInPH	C_s	2.3350	1.7229	371.2	1740.4	

and 2.049 Å for M = Al, Ga or In, respectively).[48] The planar geometry is in contrast to the *trans*-C_{2h} geometry of H_2SiSiH_2[46] and must imply a degree of π bonding, although, as noted elsewhere,[2] the barrier to inversion of NH_3 and its derivatives is so small that planarity does not of itself mean that this bonding is strong.

In the absence of an experimental sighting of molecules of the type H_2MPH_2, DFT calculations have been performed to

Table 6 $\delta_{sym}(NH_3)$ and $\delta_{sym}(PH_3)$ wavenumbers (in cm^{-1}) for some monoammonia and monophosphine adducts of metal atoms

Compound	$\delta_{sym}(NH_3)$	$\Delta\delta_{sym}(NH_3)$[a]	Ref.	Compound	$\delta_{sym}(PH_3)$	$\Delta\delta_{sym}(PH_3)$[a]	Ref.
NH_3	974.5		25	PH_3	993.8		22
$Li{\cdot}NH_3$	1133	+159	26				
$Na{\cdot}NH_3$	1079	+105	26				
$K{\cdot}NH_3$	1064	+90	26				
$Cs{\cdot}NH_3$	1049	+75	26				
$Al{\cdot}NH_3$	1131.4	+156.9	[b]	$Al{\cdot}PH_3$	974.7	−19.1	[b]
$Ga{\cdot}NH_3$	1104.2	+129.7	[b]	$Ga{\cdot}PH_3$	973.6	−20.2	[b]
$In{\cdot}NH_3$	1082.9	+108.4	[b]	$In{\cdot}PH_3$	974.4	−19.4	[b]
$Fe{\cdot}NH_3$	1131.5	+157.0	27, 28				
$Ni{\cdot}NH_3$	1132.5	+158.0	29				
$Cu{\cdot}NH_3$	1117	+143	28	$Cu{\cdot}PH_3$	970	−23.8	23
				$Cl_4Ti{\cdot}PH_3$	967	−26.8	24

[a] $\Delta\delta_{sym}(NH_3) = \delta_{sym}(NH_3)_{complex} - \delta_{sym}(NH_3)_{free\ NH_3}$. $\Delta\delta_{sym}(PH_3) = \delta_{sym}(PH_3)_{complex} - \delta_{sym}(PH_3)_{free\ PH_3}$. [b] This work.

Table 7 Calculated inversion barriers ΔE (in kJ mol^{-1})

Molecule	ΔE	Ref.
PH_3	148.2	[a]
NH_3	23.8	[a]
PH_3^+	14.2	[a]
H_2BPH_2	17.6	33
H_2AlPH_2	41.0	[a]
$HAlPH_2$	42.6	[a]
H_2GaPH_2	47.4	[a]
$HGaPH_2$	56.7	[a]
H_2InPH_2	52.5	[a]
$HInPH_2$	59.2	[a]
CH_3PH_2	153.1	33
H_2CPH_2	11.4	33
$H_2CPH_2^+$	0	34
$HCPH_2$	0	35
CH_2CHPH_2	134.5	33
$NCPH_2$	149.4	36
$OCHPH_2$	99.6	33
$HOPH_2$	188.7	36
FPH_2	226.4	36
Pentaphosphole	0	37
Phosphole	75.3	37, 38
Phosphindolizine	14.6	38

[a] This work.

Table 8 Experimental stretching wavenumbers (in cm^{-1}) and force constants (in N m^{-1}) for several $HMNH_2$, HMOH and $HMCH_3$ species (M = Al, Ga, In, Fe or Ni)

Species	ν(M–X)	ν(M–H)	f(M–X)	f(M–H)	Ref.
$HAlNH_2$	704.6	1761.7	298.2	179.0	6
$HAlPH_2$	372.8[a]	1768.2	124.0	181.2	7
$HAlCH_3$	610	1764	214.4	176.3	40
HAlOH	817.9	1743.3	417.4	175.8	42
$HGaNH_2$	668.1	1721.8	342.7	172.9	6
$HGaPH_2$	292.6[a]	1740.6	113.5	176.8	7
$HGaCH_3$	528.7	1719.7	219.2	173.1	41
HGaOH	646.4	1669.8	337.9	163.2	42
$HInNH_2$	547.4	1530.1	248.5	137.1	6
$HInPH_2$	244.0[a]	1570.4	90.1	144.3	7
$HInCH_3$	452.2[a]	1545.9	160.2	140.9	41
HInOH	548.0	1486.3	262.7	130.1	42
$HFeNH_2$	650	1717.4	311.2	171.6	27
$HFeCH_3$	521.4	1653.4	190.4	159.1	43
$H^{58}NiNH_2$	676.5	1918.1	340.7	214.2	29
$H^{58}NiCH_3$	554.9	1945.1	217.8	220.2	44
$H^{58}NiOH$	682.7	1901.0	363.9	210.4	45

[a] Calculated value.

evaluate their structures, vibrational properties and energies, with the results detailed in Table 5 and illustrated in structure **3b**. In all three cases (M = Al, Ga or In) the geometries are non-planar (conforming to C_s symmetry) incorporating a sharply pyramidal MPH_2 moiety. Very similar results have been reported previously for H_2AlPH_2 and H_2GaPH_2 on the basis of SCF calculations which nevertheless encourage the belief that the non-planar skeletons are not necessarily incompatible with significant M–P double-bond character.[49] The M–P bonds seem to be quite short, measuring 2.3379, 2.3310 and 2.5355 Å for M = Al, Ga or In, respectively, and being therefore about 0.55 Å longer than the M–N bonds in the corresponding amido derivatives.

To investigate further the nature of the bonding, each H_2MNH_2 molecule has also been optimised in the conformation where the H_2M and NH_2 planes are orthogonal to each other. The twisted conformation is a transition state with two imaginary frequencies, one for the torsion back to the planar molecule and the other for pyramidalisation of the nitrogen centre. Twisting of the molecule causes the M–N bond to be attenuated by 0.0664, 0.0207, 0.0346 and 0.0282 Å for M = B, Al, Ga or In, respectively. It has been argued elsewhere[3] that several factors keep the M–N bond short in the twisted conformation when M is a heavier Group 13 element, namely (a) the increased charge separation between M and N in the twisted structure, giving enhanced coulombic interaction, as well as enriching the s character of the M–N σ bond, and (b) donation from the nitrogen lone pair into the M–H σ* orbitals (negative hyperconjugation, evidenced by a slight lengthening of the M–H bonds in the twisted structure). Calculation of the energy of the transition state relative to the ground state of the molecule then gives an estimate of the barrier to rotation about the M–N bond, ΔE. The results included in Table 9 are consistent with those reported elsewhere,[3,33] with ΔE = 161.9, 50.6, 65.7 and 51.5 kJ mol^{-1} for M = B, Al, Ga or In, respectively.

Calculations at a similar level give energies of 39.2, 47.4 and 52.5 kJ mol^{-1} for planarisation of H_2AlPH_2, H_2GaPH_2 and H_2InPH_2, respectively. For PH_3 a value of 148.2 kJ mol^{-1} is derived, in excellent agreement with earlier theoretical estimates (146.8,[32a] 145.8[32b] and 143.9 kJ mol^{-1}[32c]), although the value determined experimentally[31] is somewhat lower (132 kJ mol^{-1}). The value for the aluminium compound is also in good agreement with an earlier estimate[33] of 42 kJ mol^{-1}; H_2BPH_2 has been reckoned previously[33,50] to have a planarisation barrier between 18 and 25 kJ mol^{-1}. The M–P/M–H bond lengths (in Å) decrease from 2.3379/1.5837, 2.3310/1.5704 and 2.5355/1.7328 for H_2MPH_2 (M = Al, Ga or In, respectively) in its lowest energy conformation (C_s symmetry) to 2.2314/1.5749, 2.2266/1.5545 and 2.4193/1.7147 for the planar conformation (C_{2v} symmetry). Simultaneously the H–P–H/H–M–H angles change from 95.7/121.4, 95.5/121.5 and 94.6/121.7 to 106.8/128.1, 107.1/130.0 and 106.1/131.0°. The barrier to rotation around the M–P bond has then been calculated for the

Table 9 Calculated geometries (distances in Å, angles in °) and barriers to rotation (ΔE in kJ mol^{-1}) of H_2MNH_2 molecules

Dimensions	H_2BNH_2		H_2AlNH_2		H_2GaNH_2		H_2InNH_2	
H–M–N–H	180	90	180	90	180	90	180	90
M–N	1.3875	1.4534	1.7790	1.7997	1.8211	1.8557	1.9703	1.9985
M–H	1.1953	1.2081	1.5811	1.5875	1.5621	1.5767	1.7252	1.7379
N–H	1.0083	1.0062	1.0100	1.0097	1.0086	1.0077	1.0169	1.0163
H–M–H	122.0	116.3	124.4	117.5	126.7	120.3	126.6	120.6
H–N–H	113.6	113.7	110.0	109.2	111.7	111.5	110.2	109.6
ΔE	161.9		50.6		65.7		51.5	

planarised species, giving $\Delta E = 65.9$, 80.1 and 65.3 kJ mol^{-1} for H_2AlPH_2, H_2GaPH_2 and H_2InPH_2, respectively. The value for Al is in excellent agreement with that reported in an earlier theoretical study (64.9 kJ mol^{-1}).[5] Each of these barriers is therefore *higher* than that calculated for the corresponding H_2MNH_2 species in its ground state, with the gallium compound again displaying the highest barrier.

MNH_2 and MPH_2. A major photodecomposition product of matrix-isolated $HMNH_2$ is the M^I amide MNH_2 (*q.v.*);[6] of the corresponding phosphide MPH_2 there has been no obvious sign to date.[3] DFT calculations have identified a global minimum corresponding to an equilibrium geometry for each of the MNH_2 molecules (M = Al, Ga or In) with a planar skeleton and C_{2v} symmetry (see structure **4a** and Table 4). The M–N bond lengths (in Å) are $AlNH_2$ 1.8131, $GaNH_2$ 1.8840, and $InNH_2$ 2.0389, and the simulated vibrational properties generally mirror well the IR spectra associated with these molecules. By contrast, the corresponding phosphides have pyramidal skeletons and C_s symmetry (see structure **4b** and Table 5); the M–P bond lengths (in Å) are $AlPH_2$ 2.4490, $GaPH_2$ 2.4829, and $InPH_2$ 2.6962, *i.e.* about 0.63 Å longer on average than the M–N lengths.

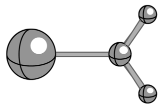

4a (MNH_2)

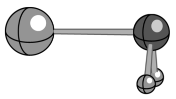

4b (MPH_2)

H_2MNH and H_2MPH. Photolysis of the metal atom adduct $M{\cdot}PH_3$ at $\lambda = ca.$ 440 nm gives not one but two insertion products, namely $HMPH_2$ and the metal(III) species H_2MPH where the odd electron is mainly confined to the phosphorus atom. No nitrogen analogue of the second tautomer has so far been reported in more than hypothetical terms.[3] Theoretical (DFT) investigations indicate (i) that H_2MNH molecules have C_s symmetry in their ground states with a slightly non-planar H_2MN unit (structure **5a**), in keeping with the results of earlier studies of H_2AlNH,[3] and (ii) that H_2MPH molecules have a similar structure with an essentially planar H_2MP unit but with the P–H bond so oriented as to give only C_1 symmetry (structure **5b**). The M–N/M–P distances (in Å and in the order M = Al, Ga or In) are 1.7603/2.3523, 1.8545/2.3421 and 2.0146/2.5554, little different from those in corresponding molecules of the types H_2MNH_2/H_2MPH_2. The vibrational properties calculated for H_2MPH are wholly consistent with the IR spectra attributed to these molecules for M = Al, Ga or In.[7]

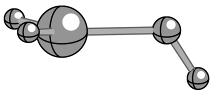

5a (H_2MNH)

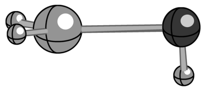

5b (H_2MPH)

The main difference between H_2MNH and H_2MPH lies in their energies with respect to the relevant $HMNH_2$ and $HMPH_2$ isomers. H_2MNH is a high-energy species lying +125, +134.6, and +159.6 kJ mol^{-1} above $HMNH_2$ for M = Al, Ga or In, respectively. By contrast, the energy difference between H_2MPH and $HMPH_2$ is estimated to be only +1.4 (M = Al), +19.9 (M = Ga), and +52.6 kJ mol^{-1} (M = In). Earlier calculations at the TZ2P CCSD level even put H_2AlPH slightly *lower* in energy than $HAlPH_2$.[5] With both H_2MNH and H_2MPH there is but a small barrier to rotation about the M–N or M–P bond (<2 kJ mol^{-1}).

ME, HMEH and $H_3M{\cdot}EH_3$. There is very little experimental information but for the purpose of comparison the present DFT analysis has been extended to include molecules of these types.

Given the technical importance of the materials in bulk,[1] there is a surprising dearth of information about the diatomic molecules ME. However, where checks can be made, the results of the DFT calculations on ME molecules in their $^3\Pi$ ground states (see Tables 4 and 5) are in satisfactory agreement with the limited experimental findings reported so far. M–N/M–P distances are calculated to be (in the order M = Al, Ga and In) 1.8001/2.2290, 1.8640/2.2616 and 2.0256/2.4662 Å (*cf.* r_e(Al–N) estimated experimentally to be 1.7864 Å[51]). The corresponding M–N/M–P vibrational frequencies are calculated to be 742.9/454.8, 586.2/345.7 and 501.2/280.2 cm^{-1}. For comparison, ω_e for gaseous AlN has been estimated by experiment[52] to be 746.9 cm^{-1} and the stretching frequencies of ^{69}GaP[52] and InP[53] each isolated in an argon matrix are reported to be 283.6 and 257.9 cm^{-1}, respectively.

The calculations of this study also confirm that HMEH molecules are invariably high-energy species, being less stable than the MEH_2 isomer by 177.7 (Al), 188.4 (Ga) and 257.5 kJ mol^{-1} (In) for E = N, and by 43.5 (Al), 69.6 (Ga) and 183.1 kJ mol^{-1} (In) for E = P. The geometries are consistently bent with H–M–E angles of 167.2, 141.9 and 135.9° (E = N) or 177.1, 177.3 and 114.7° (E = P), and M–E–H angles of 157.4, 140.7 and 136.9° (E = N) or 84.3, 85.9 and 94.8° (E = P), as registered in Tables 4 and 5, although the potential well is extremely shallow with respect to the bending coordinates. At 1.6271/2.1535 Å (Al–N/Al–P), 1.6989/2.1445 Å (Ga–N/Ga–P) and 1.8345/2.3350 Å (In–N/In–P) the M–E bond distances are calculated to be shorter than in any other compound with the general formula H_mMEH_n (m, n = 0–3). An earlier tentative assignment[54] of IR bands to matrix-isolated HAlNH has subsequently been questioned,[6] and on the evidence of published work it is doubtful whether this molecule, or any homologue of the heavier Group 13/15 elements, has yet been sighted in the laboratory.

Molecules of the type $H_3M{\cdot}EH_3$ are ammonia or phosphine complexes of alane, gallane or indane some of which have attracted earlier quantum chemical investigations;[55] matrix evidence of the species $H_3Ga{\cdot}NH_3$[56] and $H_3Ga{\cdot}PH_3$[57] has been found, but otherwise experiment has little to offer. According to DFT calculations, the M–E distances (in Å) are, as expected,

Table 10 Estimated π-bond energies (ΔE in kJ mol^{-1}) for selected molecules[a]

Group 13 derivative	ΔE	Ref.	Group 14 derivative	ΔE	Ref.	Group 15 derivative	ΔE	Ref.
$HBCH_2$	225	62	H_2CCH_2	272[b]	63			
H_2BNH_2	162	[c]						
$HBNH_2$	150	[c,d]						
H_2BPH_2	170	44						
$HBSiH_2$	113	62						
$HAlCH_2$	39	62	H_2SiSiH_2	106–127	46	HPPH	141	64
H_2AlNH_2	51	[c]	H_2SiCH_2	149	46	$HPCH_2$	180	32
H_2AlPH_2	66	[c]	H_2SiNH	159	46	$[H_2PCH_2]^+$	131	33
$HAlNH_2$	39	[c]				HPNH	167–188	65
$HAlPH_2$	48	[c]				$HPSiH_2$	142	66
$HAlSiH_2$	59	62						
H_2AlOH	15	67						
H_2AlSH	31	67						
H_2GaNH_2	66	[c]	H_2GeGeH_2	106	68	HAsAsH	98	69
H_2GaPH_2	80	[c]	H_2GeCH_2	135	68	$HAsCH_2$	160	70
$HGaNH_2$	38	[c]				$HAsSiH_2$	126	66
$HGaPH_2$	35	[c]						
H_2GaSH	35	67						
H_2InNH_2	52	[c]	H_2SnSnH_2	82	68	HSbSbH	69	69
H_2InPH_2	65	[c]	H_2SnCH_2	87	68	$HSbCH_2$	123	70
$HInNH_2$	31	[c]						
$HInPH_2$	24	[c]						
						HBiBiH	59	69
						$HBiCH_2$	110	71

[a] Unless indicated otherwise, ΔE was estimated by quantum chemical calculations, usually in terms of the barrier to rotation about the putative multiple bond. [b] Determined experimentally. [c] This work. [d] In this calculation the H–B–N angle was constrained to the value in the planar optimised molecule (124.8°).

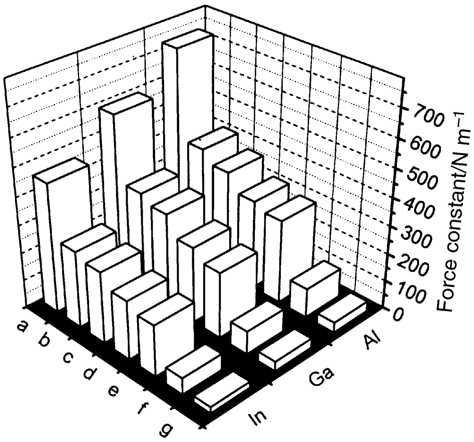

Fig. 1 Plot of the force constants f(MN) of compounds with the general formula H_mMNH_n (M = Al, Ga or In; $m, n = 0$–3): (a) HMNH, (b) H_2MNH_2, (c) $HMNH_2$, (d) MNH_2, (e) MN, (f) $H_3M{\cdot}NH_3$, and (g) $M{\cdot}NH_3$.

relatively long: $H_3Al{\cdot}NH_3$ 2.0931; $H_3Ga{\cdot}NH_3$ 2.1795; $H_3In{\cdot}NH_3$ 2.3788; $H_3Al{\cdot}PH_3$ 2.5771; $H_3Ga{\cdot}PH_3$ 2.6012; and $H_3In{\cdot}PH_3$ 2.9351. Other dimensions are listed in Tables 4 and 5.

Discussion

The calculations described in the preceding section indicate that, for a given metal M = Al, Ga or In, the M–N distances in molecules of the general type H_mMNH_n follow the order $M{\cdot}NH_3 > H_3M{\cdot}NH_3 > MNH_2 > MN > HMNH_2 \gtrsim H_2MNH \approx H_2MNH_2 > HMNH$. The M–N stretching force constants, based where possible on experimental data, vary in the orders (i) $HMNH \gg H_2MNH_2 \approx H_2MNH > HMNH_2 > MNH_2 > MN \gg H_3M{\cdot}NH_3 \gg M{\cdot}NH_3$, and (ii) $M = B \gg Al > Ga > In$ for a given family of H_mMNH_n molecules (see Fig. 1, for example). Despite the structural differences between many of the phosphine derivatives and their ammonia counterparts, M–P distances follow a pattern broadly similar to that of the M–N distances, namely $M{\cdot}PH_3 > H_3M{\cdot}PH_3 > MPH_2 > HMPH_2 \gtrsim H_2MPH \gtrsim H_2MPH_2 > MP > HMPH$, the sole exception being the position of the diatomic MP which is now second only to HMPH in the shortness of its bond. The low symmetry of many of the phosphorus molecules and the scarcity of experimental data combine to deny a useful role to the M–P stretching force constant as a reporter on the bonding.

M–H distances consistently vary in the order $HMEH_2 \gtrsim H_3M{\cdot}EH_3 > H_2MEH \approx H_2MEH_2 > HMEH$ for a given metal, while M–H stretching force constants vary in the opposite sense. Unlike the M–E bonds which invariably lengthen in the sequence Al < Ga < In, M–H bonds mostly conform to the pattern Al > Ga < In. This ability of Ga^{III} to better Al^{III} in the strength of the bonds it forms to hydrogen is also evident from the frequencies of the M–H stretching modes (and the associated force constants) which typically run in the order Al < Ga > In.[39]

Of the planar or pseudo-planar ammonia derivatives $HMNH_2$, H_2MNH_2 and H_2MNH which feature relatively short M–N bonds, only the first two exhibit appreciable barriers to rotation, ΔE, about the M–N bond, with ΔE taking values in the ranges 31–150 and 50–162 kJ mol^{-1} for $HMNH_2$ and H_2MNH_2, respectively, where M = B, Al, Ga or In. If ΔE is taken to be a lower limit to the π-bond strength, the following observations may be made.

(i) Despite having a relatively short M–N bond (little different from that in H_2MNH_2), radicals of the type H_2MNH have little or no M–N π bonding.

(ii) π Bonding adds significantly to the strength of the M–N bond only in the cases of $HBNH_2$ and H_2BNH_2.

(iii) For all the heavier Group 13 elements the π interaction in molecules of the types $HMNH_2$ and H_2MNH_2 is quite weak but

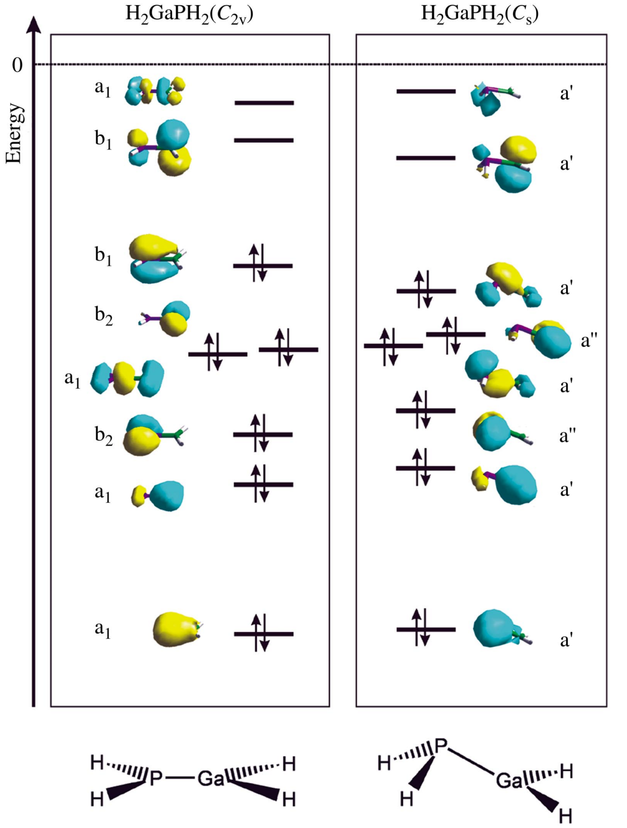

Fig. 2 Frontier orbitals of H$_2$GaPH$_2$ in the energy-minimum geometry (C_s symmetry) and the planar geometry (C_{2v} symmetry).

varies in the order $\mathrm{B} \gg \mathrm{Al} < \mathrm{Ga} > \mathrm{In}$; gallium is out of line with its neighbours, showing a modest return to the behaviour of boron.

(iv) The estimated Δ*E* values in HMNH$_2$ and H$_2$MNH$_2$ molecules where M = Al, Ga or In are larger than those in the singly bonded molecules H$_3$CCH$_3$ (12 kJ mol^{-1}),[58] H$_2$N-NH$_2$ (25 kJ mol^{-1}),[59] H$_3$GeGeH$_3$ (5 kJ mol^{-1}),[60] and H$_2$PPH$_2$ (9–11 kJ mol^{-1}),[61] but not always by a substantial margin.

(v) The π-bond energies in HMNH$_2$ and H$_2$MNH$_2$ molecules naturally invite comparison with those in other molecules with the potential for multiple bonding between elements from Groups 13–15;[2] Table 10 includes some representative estimates, mostly based on calculations. Hence H$_2$AlNH$_2$ has a π-bond energy (*ca.* 51 kJ mol^{-1}) estimated to be less than 40% that of the isoelectronic species H$_2$SiCH$_2$ (149 kJ mol^{-1})[46] and [H$_2$PCH$_2$]$^+$ (131 kJ mol^{-1}).[33] Similar to H$_2$AlNH$_2$ in π-bond energy are HAlCH$_2$ (39 kJ mol^{-1})[62] and HAlSiH$_2$ (59 kJ mol^{-1}),[62] whereas the corresponding energies for the chalcogenide derivatives H$_2$AlOH (15 kJ mol^{-1})[67] and H$_2$AlSH (31 kJ mol^{-1})[67] are even smaller. Whatever the *potential* for dative ligand→metal π bonding, therefore, the calculations add further weight to the view[2] that this interaction is weak and of secondary importance to the metal–ligand bond. The properties of H$_2$MNH (see above) serve to emphasise this point.

The phosphine derivatives HMPH$_2$ and H$_2$MPH$_2$ differ conspicuously from their amide analogues in having not a planar but a pyramidal MPH$_2$ unit. This disparity has its roots in the inversion barrier of the parent molecule PH$_3$ which at *ca.* 140 kJ mol^{-1} is nearly six times bigger than the corresponding barrier of NH$_3$ (24 kJ mol^{-1}).[31]

It follows that replacement of a hydrogen in PH$_3$ by another substituent X will lead to a planar XPH$_2$ skeleton only in the event of strong P–X π bonding. Significantly, the inversion barriers in the molecules HMPH$_2$ and H$_2$MPH$_2$ are only about one-third the value for free PH$_3$, suggesting that there is appreciable stabilisation of the planar transition state. This is also evident in the MO schemes shown in Figs. 2 and 3. The frontier

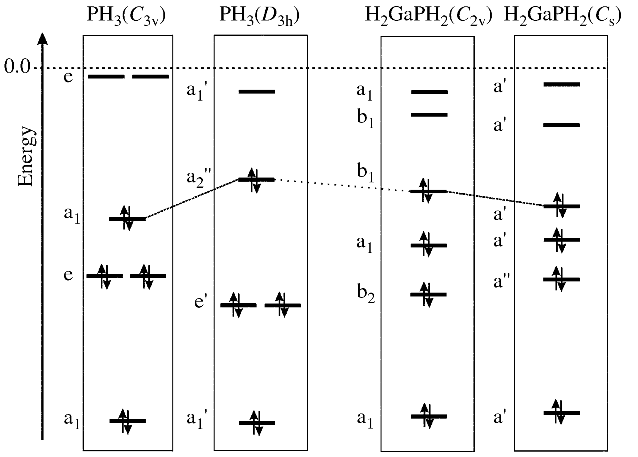

Fig. 3 Energies of the frontier orbitals of PH$_3$ correlating with those of H$_2$GaPH$_2$ in the energy-minimum (C_{3v} and C_s symmetries) and planar geometries (D_{3h} and C_{2v} symmetries).

orbitals of PH$_3$ have energies (in eV) of −16.115 (a$_1$), −9.470 (e), −6.878 (a$_1$, HOMO) and −0.347 (e$_1$, LUMO) for the molecule in C_{3v} symmetry and −16.252 (a$_1$′), −10.73 (e$_1$′), −5.057 (a$_2$″, HOMO) and −1.159 (a$_1$′, LUMO) in planar (D_{3h}) symmetry. Thus the HOMO is destabilised by 1.821 eV in the planar D_{3h} form relative to the pyramidal C_{3v} form. In the case of H$_2$GaPH$_2$ the frontier orbitals have energies (in eV) of −15.744 (a′), −9.661 (a″), −7.842 (a′), −6.352 (a′, HOMO), −2.589 (a′, LUMO) and −0.760 (a′) for the molecule in C_s symmetry and −15.893 (a$_1$), −10.296 (b$_2$), −8.154 (a$_1$), −5.572 (b$_1$, HOMO), −2.169 (b$_1$, LUMO) and −1.066 (a$_1$) in the planar form with C_{2v} symmetry. Thus the HOMO in the planar molecule is destabilised by only 0.78 eV, a factor of 2.3 less than for PH$_3$. In terms of the second-order Jahn–Teller effect any stabilisation of H$_2$GaPH$_2$ in the planar (C_{2v}) form must depend not on the ability of a distortion to mix the HOMO and the LUMO since both now span the same irreducible representation (b$_1$). Instead the distortion must cause a mixing of the HOMO with the LUMO-1 (a$_1$) which is close in energy to the a$_1$′ LUMO of PH$_3$ in its planar (D_{3h}) configuration (see Fig. 3). That the HOMO in planar H$_2$GaPH$_2$ is lowered in energy with respect to that in planar PH$_3$, as a result of π-bonding and other effects, means that the HOMO–LUMO-1 gap in the former is 0.515 eV *greater* than the HOMO–LUMO gap in the latter. Accordingly there is a corresponding energetic disadvantage in pyramidalisation of the gallaphosphine as compared with the parent phosphine molecule.

Earlier theoretical studies have indeed shown that compounds containing *planar* three-coordinated phosphorus are good π-type electron-pair donors.[33] Strong π-electron-pair acceptors may be expected therefore to stabilise the planar structure, as demonstrated by calculations which forecast planar ground-state structures for [H$_2$PCH$_2$]$^+$ [34] and HCPH$_2$.[35] In pseudo-aromatic systems, too, phosphorus can be found in a trigonal planar environment, *e.g.* 1-[bis(trimethylsilyl)methyl]-3,5-bis(trimethylsilyl)-1,2,4-triphosphole, the nucleus of which is a planar five-membered ring.[72] Accordingly, we have calculated the barrier to rotation around the M–P bond in the *planarised* forms of the molecules HMPH$_2$ and H$_2$MPH$_2$. The resulting estimates of Δ*E* in the two series are striking for being consistently higher than the corresponding parameters for the molecules HMNH$_2$ and H$_2$MNH$_2$ (see Table 10), implying that M–P π bonding is somewhat stronger than M–N π bonding. By contrast, H$_2$MPH molecules resemble H$_2$MNH in their minuscule barriers to rotation (<2 kJ mol^{-1}); although the M–P distances are intermediate between those of HMPH$_2$ and H$_2$MPH$_2$ in their ground state structures, they are substantially longer when compared with those of the planarised molecules.

Acknowledgements

The authors thank (i) the EPSRC for support of this research, including the purchase of equipment and the award of an Advanced Fellowship to T. M. G., and (ii) the Deutsche Forschungsgemeinschaft for the award of a postdoctoral grant to H.-J. H.

References

1 *Chemistry of Aluminium, Gallium, Indium and Thallium*, ed. A. J. Downs, Blackie, Glasgow, 1993.

2 P. P. Power, *Chem. Rev.*, 1999, **99**, 3463; W. H. Fink, P. P. Power and T. L. Allen, *Inorg. Chem.*, 1997, **36**, 1431.

3 R. D. Davy and K. L. Jaffrey, *J. Phys. Chem.*, 1994, **98**, 8930.

4 S. Sakai, *J. Phys. Chem.*, 1992, **96**, 8369.

5 R. D. Davy and H. F. Schaefer, III, *J. Phys. Chem. A*, 1997, **101**, 3135.

6 H.-J. Himmel, A. J. Downs and T. M. Greene, *Chem. Commun.*, 2000, 871; *J. Am. Chem. Soc.*, 2000, **122**, 9793.

7 H.-J. Himmel, A. J. Downs and T. M. Greene, *Inorg. Chem.*, 2000, **40**, 396.

8 B. S. Jursic, *J. Mol. Struct.* (*THEOCHEM*), 1998, **428**, 61.

9 M. J. Frisch, G. W. Trucks, H. B. Schlegel, G. E. Scuseria, M. A. Robb, J. R. Cheeseman, V. G. Zakrzewski, J. A. Montgomery, Jr., R. E. Stratmann, J. C. Burant, S. Dapprich, J. M. Millam, A. D. Daniels, K. N. Kudin, M. C. Strain, O. Farkas, J. Tomasi, V. Barone, M. Cossi, R. Cammi, B. Mennucci, C. Pomelli, C. Adamo, S. Clifford, J. Ochterski, G. A. Petersson, P. Y. Ayala, Q. Cui, K. Morokuma, D. K. Malick, A. D. Rabuck, K. Raghavachari, J. B. Foresman, J. Cioslowski, J. V. Ortiz, B. B. Stefanov, G. Lui, A. Liashenko, P. Piskorz, I. Komaromi, R. Gomperts, R. L. Martin, D. J. Fox, T. Keith, M. A. Al-Laham, C. Y. Peng, A. Nanayakkara, C. Gonzalez, M. Challacombe, P. M. W. Gill, B. G. Johnson, W. Chen, M. W. Wong, J. L. Andres, M. Head-Gordon, E. S. Replogle and J. A. Pople, GAUSSIAN 98, Revision A.3, Gaussian Inc., Pittsburgh, PA, 1998.

10 C. Fonseca Guerra, J. G. Snijders, G. Te Velde and E. J. Baerends, *Theor. Chim. Acta*, 1998, **99**, 391.

11 S. H. Vosko, L. Wilk and M. Nusair, *Can. J. Phys.*, 1980, **58**, 1200.

12 A. D. Becke, *Phys. Rev. A*, 1988, **38**, 3098.

13 J. P. Perdew, *Phys. Rev. B*, 1986, **33**, 8822.

14 J. P. Perdew, *Phys. Rev. B*, 1986, **34**, 7406.

15 ASYM 40, version 3.0, upgrade of program ASYM 20, L. Hedberg and I. M. Mills, *J. Mol. Spectrosc.*, 1993, **160**, 117.

16 D. M. Dennison, *Rev. Mod. Phys.*, 1940, **12**, 175; G. E. Hansen and D. M. Dennison, *J. Chem. Phys.*, 1952, **20**, 313.

17 C. R. Pulham, A. J. Downs, M. J. Goode, T. M. Greene and I. M. Mills, *Spectrochim. Acta*, *Part A*, 1995, **51**, 769.

18 H.-J. Himmel, A. J. Downs and T. M. Greene, *J. Am. Chem. Soc.*, 2000, **122**, 922.

19 *CRC Handbook of Chemistry and Physics*, ed.-in-chief D. R. Lide, CRC Press, Boca Raton, FL, 80th edn., 1999–2000.

20 H.-J. Himmel, A. J. Downs and T. M. Greene, unpublished results.

21 H.-J. Himmel, A. J. Downs, J. C. Green and T. M. Greene, *J. Phys. Chem. A*, 2000, **104**, 3642.

22 R. T. Arlinghaus and L. Andrews, *J. Chem. Phys.*, 1984, **81**, 4341.

23 G. A. Bowmaker, *Aust. J. Chem.*, 1978, **31**, 2549.

24 J. B. Everhart and B. S. Ault, *Inorg. Chem.*, 1996, **35**, 4090.

25 See, for example, S. Süzer and L. Andrews, *J. Chem. Phys.*, 1987, **87**, 5131; L. Abouaf-Marguin, M. E. Jacox and D. E. Milligan, *J. Mol. Spectrosc.*, 1977, **67**, 34.

26 S. Süzer and L. Andrews, *J. Am. Chem. Soc.*, 1987, **109**, 300.

27 J. W. Kauffman, R. H. Hauge and J. L. Margrave, *High Temp. Sci.*, 1984, **17**, 237.

28 J. Szczepanski, M. Szczesniak and M. Vala, *Chem. Phys. Lett.*, 1989, **162**, 123.

29 D. W. Ball, R. H. Hauge and J. L. Margrave, *High Temp. Sci.*, 1988, **25**, 95.

30 J. D. Swalen and J. A. Ibers, *J. Chem. Phys.*, 1962, **36**, 1914.

31 R. E. Weston, Jr., *J. Am. Chem. Soc.*, 1954, **76**, 2645.

32 (*a*) P. Schwerdtfeger, L. J. Laakhonen and P. Pyykkö, *J. Chem. Phys.*, 1992, **96**, 6807; (*b*) R. Ahlrichs, F. Keil, H. Lischka, W. Kutzelnigg and V. Staemmler, *J. Chem. Phys.*, 1975, **63**, 455; (*c*) D. S. Marynick and D. A. Dixon, *J. Phys. Chem.*, 1982, **86**, 914.

33 C. Schade and P. v. R. Schleyer, *J. Chem. Soc.*, *Chem. Commun.*, 1987, 1399.

34 J. Kapp, C. Schade, A. M. El-Nahasa and P. v. R. Schleyer, *Angew. Chem.*, *Int. Ed. Engl.*, 1996, **35**, 2236.

35 M. T. Nguyen, M. A. McGinn and A. F. Hegarty, *Inorg. Chem.*, 1986, **25**, 2185.

36 S. Yabushita and M. S. Gordon, *Chem. Phys. Lett.*, 1985, **117**, 321.

37 M. N. Glukhotsev, A. Drunsfeld and P. v. R. Schleyer, *J. Phys. Chem.*, 1996, **100**, 13447.

38 L. Nyulászi, U. Bergsträßer, M. Regitz and P. v. R. Schleyer, *New J. Chem.*, 1998, 651.

39 P. Pullumbi, C. Mijoule, L. Manceron and Y. Bouteiller, *Chem. Phys.*, 1994, **185**, 13; P. Pullumbi, C. Mijoule, L. Manceron and Y. Bouteiller, *Chem. Phys.*, 1994, **185**, 25.

40 J. M. Parnis and G. A. Ozin, *J. Phys. Chem.*, 1989, **93**, 1204; J. M. Parnis and G. A. Ozin, *J. Phys. Chem.*, 1989, **93**, 1220; R. D. Lafleur and J. M. Parnis, *J. Phys. Chem.*, 1992, **96**, 2429.

41 H.-J. Himmel, A. J. Downs, T. M. Greene and L. Andrews, *Chem. Commun.*, 1999, 2243; H.-J. Himmel, A. J. Downs, T. M. Greene and L. Andrews, *Organometallics*, 2000, **19**, 1060.

42 R. H. Hauge, J. W. Kauffman and J. L. Margrave, *J. Am. Chem. Soc.*, 1980, **102**, 6005.

43 W. E. Billups, M. M. Konarski, R. H. Hauge and J. L. Margrave, *J. Am. Chem. Soc.*, 1980, **102**, 7393; G. A. Ozin and J. G. McCaffrey, *J. Am. Chem. Soc.*, 1982, **104**, 7351; G. A. Ozin and J. G. McCaffrey, *Inorg. Chem.*, 1983, **22**, 1397.

44 S.-C. Chang, R. H. Hauge, W. E. Billups and J. L. Margrave, *Inorg. Chem.*, 1988, **27**, 205.

45 M. Park, R. H. Hauge and J. L. Margrave, *High Temp. Sci.*, 1988, **25**, 1.

46 M. W. Schmidt, P. N. Truong and M. S. Gordon, *J. Am. Chem. Soc.*, 1987, **109**, 5217.

47 J. D. Carpenter and B. S. Ault, *J. Phys. Chem.*, 1991, **95**, 3502.

48 G. M. Sheldrick and W. S. Sheldrick, *J. Chem. Soc. A*, 1969, 2279; K. M. Waggoner, M. M. Olmstead and P. P. Power, *Polyhedron*, 1990, **9**, 257.

49 T. J. Dudley, W. W. Brown and M. R. Hoffmann, *J. Phys. Chem. A*, 1999, **103**, 5152.

50 T. L. Allen, A. C. Scheiner and H. F. Schaefer, III, *Inorg. Chem.*, 1990, **29**, 1930; M. B. Coolidge and W. T. Borden, *J. Am. Chem. Soc.*, 1990, **112**, 1704.

51 J. D. Simons and J. K. McDonald, *J. Mol. Spectrosc.*, 1972, **41**, 584.

52 S. Li, R. J. Van Zee and W. Weltner, Jr., *J. Phys. Chem.*, 1993, **97**, 11393.

53 S. Li, R. J. Van Zee and W. Weltner, Jr., *J. Phys. Chem.*, 1994, **98**, 2275.

54 D. V. Lanzisera and L. Andrews, *J. Phys. Chem. A*, 1997, **101**, 5082.

55 J. Chey, H.-S. Choe, Y.-M. Chook, E. Jensen, P. R. Seida and M. M. Franci, *Organometallics*, 1990, **9**, 2309; C. M. B. Marsh, T. P. Hamilton, Y. Xie and H. F. Schaefer, III, *J. Chem. Phys.*, 1992, **96**, 5310; P. Jungwirth and R. Zahradník, *J. Mol. Struct.* (*THEOCHEM*), 1993, **283**, 317; M. Chaillet, A. Dargelos and C. J. Marsden, *New J. Chem.*, 1994, **18**, 693.

56 E. Johnsen, D. Phil. Thesis, University of Oxford, 2000.

57 C. R. Pulham, A. J. Downs, M. J. Goode, D. W. H. Rankin and H. E. Robertson, *J. Am. Chem. Soc.*, 1991, **113**, 5149; C. R. Pulham, D. Phil. Thesis, University of Oxford, 1991.

58 D. R. Lide, Jr., *J. Chem. Phys.*, 1958, **29**, 1426.

59 N. Ohashi, W. J. Lafferty and W. B. Olson, *J. Mol. Spectrosc.*, 1986, **117**, 119.

60 D. A. Dows and R. M. Hexter, *J. Chem. Phys.*, 1956, **24**, 1029.

61 J.-B. Robert, H. Marsmann and J. R. Van Wazer, *Chem. Commun.*, 1970, 356.

62 P. v. R. Schleyer and D. Kost, *J. Am. Chem. Soc.*, 1988, **110**, 2105.

63 J. E. Douglas, B. S. Rabinovitch and F. S. Looney, *J. Chem. Phys.*, 1955, **23**, 315.

64 T. L. Allen, A. C. Scheiner, Y. Yamaguchi and H. F. Schaefer, III, *J. Am. Chem. Soc.*, 1986, **108**, 7579.

65 G. Trinquier, *J. Am. Chem. Soc.*, 1982, **104**, 6969.

66 M. Driess and R. Janoschek, *J. Mol. Struct.* (*THEOCHEM*), 1994, **313**, 129.

67 W. H. Fink, P. P. Power and T. L. Allen, *Inorg. Chem.*, 1997, **36**, 1431.

68 T. L. Windus and M. S. Gordon, *J. Am. Chem. Soc.*, 1992, **114**, 9559.

69 S. Nagase, S. Suzuki and T. Kurakake, *J. Chem. Soc.*, *Chem. Commun.*, 1990, 1724.

70 K. D. Dobbs, J. E. Boggs and A. H. Cowley, *Chem. Phys. Lett.*, 1987, **141**, 372.

71 L. Weber, *Chem. Ber.*, 1996, **129**, 367.

72 F. G. N. Cloke, P. B. Hitchcock, P. Hunnable, J. F. Nixon, L. Nyulászi, E. Niecke and V. Thelen, *Angew. Chem.*, *Int. Ed.*, 1998, **37**, 1083.